A PERTURBATION SOLUTION OF ROTOR FLAPPING STABILITY

Wayne Johnson

Army Air Mobility Research and Development Laboratory
Moffett Field, California

September 1972

A PERTURBATION SOLUTION OF ROTOR FLAPPING STABILITY

by
Wayne Johnson

U.S. Army Air Mobility R&D Laboratory
Moffett Field, Calif., 94035

AIAA ATMOSPHERIC FLIGHT MECHANICS CONFERENCE

September 11-13, 1972

Ames Research Center
Moffett Field, Calif.

A PERTURBATION SOLUTION OF ROTOR FLAPPING STABILITY

Wayne Johnson*

U.S. Army Air Mobility R&D Laboratory
Moffett Field, California 94035

Abstract

The stability of the flapping motion of a single blade of a helicopter rotor is examined using the techniques of perturbation theory. The equation of motion studied is linear, with periodic aerodynamic coefficients due to the forward speed of the rotor. Blade pitch feedback proportional to both flapping displacement (δ_3) and flapping rate is included. Four cases are considered: small and large advance ratio, and small and large Lock number. The solution of this problem demonstrates the information which may be obtained using perturbation techniques. This paper discusses mainly the results of the analysis rather than the mathematics of their derivation, with primary emphasis on the eigenvalues (i.e., root loci) as indicators of the system stability and response. The small advance ratio results in particular are very useful, being valid out to an advance ratio of about 0.5. It is concluded that perturbation theory is a powerful mathematical technique which should prove very useful in analyzing some of the problems of helicopter dynamics.

Nomenclature

K_P	flap proportional feedback gain
K_R	flap rate feedback gain
M_β	aerodynamic moment due to flapping displacement
$M_{\dot\beta}$	aerodynamic moment due to flapping rate
M_θ	aerodynamic moment due to blade pitch
LHP	left-hand plane
RHP	right-hand plane
LHS	left-hand side
RHS	right-hand side
Re	real part of a complex number
Im	imaginary part of a complex number
β	flap motion degree of freedom
γ	blade Lock number
λ	eigenvalue or root of the system
μ	rotor advance ratio (forward speed divided by rotor tip speed)
ν	rotating natural frequency of flap motion (centrifugal and structural stiffening), nondimensionalized with rotor rotational speed
ψ	rotor azimuth angle, measured from downstream
$O(\ )$	"the order of"
$\overline{(\ )}$	conjugate of a complex number

Introduction

This paper considers the application of perturbation techniques to helicopter rotor dynamics. Perturbation theory has been well developed in recent years, but has not found much application to rotary wing problems. Classically helicopter engineering has made use of the same perturbation theories that fixed wing engineering has, for example lifting line theory and engineering beam theory (both require a large blade aspect ratio). Another classical example is actuator disk theory (a large number of blades is required). These theories were developed on an intuitive basis however, and the more rigorous mathematical techniques of perturbation theory have not yet found widespread use for rotary wings. The classical applications are largely for aerodynamic problems; the mathematics of those problems can be very complicated however because the equations involved are highly nonlinear partial differential equations. The treatment of dynamic problems can be more tractable since only ordinary differential equations are involved. Problems with constant coefficient linear differential equations can be solved exactly with well established methods, so for these problems the extra effort of perturbation theory may not be justified. On the other hand for problems with time varying or nonlinear differential equations the only solution procedure generally applicable is the numerical integration of the equations of motion. However, purely numerical solutions are not entirely satisfactory for obtaining an understanding of the physical character of the system, or for formulating general design rules. Furthermore, an analytic solution for the general case would be difficult to obtain (if possible at all) and would be so complex as to be hardly better than the numerical solution. The only systems that can be practicably handled analytically are those involving linear constant coefficient differential equations. Perturbation techniques are available which are methods to study time varying or nonlinear systems such that at each step in the analysis only linear constant coefficient equations must be handled. Time varying or nonlinear differential equations are characteristic features of helicopter dynamics and aerodynamics, primarily due to the rotation of the wing. Thus the possibilities for

*Research Scientist

the use of perturbation theory in rotary wing problems are very extensive.

This paper considers the stability of the flapping motion of a single blade of a helicopter rotor. This is a single degree of freedom, second-order system, with analytic aerodynamic coefficients. The governing equation is linear with time varying coefficients; it is given below.

$$\ddot{\beta} + \nu^2\beta = \gamma\left[(M_{\dot{\beta}} - K_R M_\theta)\dot{\beta} + (M_\beta - K_P M_\theta)\beta\right] \tag{1}$$

where the aerodynamic coefficients are

$$M_{\dot{\beta}} = \begin{cases} -\left(\frac{1}{8} + \frac{1}{6}\mu\sin\psi\right) & \text{(i)} \\ -\left[\frac{1}{8} + \frac{1}{6}\mu\sin\psi + \frac{1}{12}(\mu\sin\psi)^4\right] & \text{(ii)} \\ \frac{1}{8} + \frac{1}{6}\mu\sin\psi & \text{(iii)} \end{cases}$$

Region

$$M_\beta = \begin{cases} -\mu\cos\psi\left(\frac{1}{6} + \frac{1}{4}\mu\sin\psi\right) & \text{(i)} \\ -\mu\cos\psi\left[\frac{1}{6} + \frac{1}{4}\mu\sin\psi - \frac{1}{6}(\mu\sin\psi)^3\right] & \text{(ii)} \\ \mu\cos\psi\left(\frac{1}{6} + \frac{1}{4}\mu\sin\psi\right) & \text{(iii)} \end{cases}$$

$$M_\theta = \begin{cases} \frac{1}{8} + \frac{1}{3}\mu\sin\psi + \frac{1}{4}(\mu\sin\psi)^2 & \text{(i)} \\ \frac{1}{8} + \frac{1}{3}\mu\sin\psi + \frac{1}{4}(\mu\sin\psi)^2 - \frac{1}{12}(\mu\sin\psi)^4 & \text{(ii)} \\ -\left[\frac{1}{8} + \frac{1}{3}\mu\sin\psi + \frac{1}{4}(\mu\sin\psi)^2\right] & \text{(iii)} \end{cases}$$

and the three regions are defined by

region (i): $0 < \mu\sin\psi < \mu$

region (ii): $-1 < \mu\sin\psi < 0$

region (iii): $-\mu < \mu\sin\psi < -1$

This is the homogeneous equation for small perturbations of the flapping motion of the blade about an equilibrium state; the derivation of this equation may be found in the literature.[1] β is the degree of freedom representing the blade flapping motion perturbation. The equation is nondimensionalized with the rotor speed, so the time variable is the azimuth angle ψ. ν is the rotating natural frequency (nondimensionalized with the rotor speed) of the flapping motion, which may be greater than 1.0 for flapping hinge offset or cantilever root restraint of the blade. γ is the Lock number, defined by $\gamma = \rho acR^4/I_b$ (ρ is the air density, a the two-dimensional lift curve slope, c the blade chord, and R the blade radius); I_b is the equivalent mass of the flapping motion, given by the integral over the span of the square of the mode shape of the flapping motion weighted by the mass per unit length of the blade; for the rigid flapping motion of an articulated blade, the mode shape is proportional to the radial distance from the hinge, and so I_b is just the moment of inertia of the blade about the flapping hinge. K_P is the flap proportional feedback gain, better known as tan δ_3; K_R is the flap proportional feedback gain. A feedback law $\Delta\theta = -K_P\beta - K_R\dot{\beta}$ has been used ($\Delta\theta$ is the blade pitch change due to flapping feedback control). μ is the rotor advance ratio (forward velocity divided by rotor tip speed). The coefficients M_β, $M_{\dot{\beta}}$, and M_θ are the aerodynamic forces on the blade, hence their multiplication by γ and their dependence on μ. The three regions for the coefficients reflect the influence of the reverse flow region of the rotor disk. In region (i) there is normal flow over the entire blade span; in region (iii) reverse flow over the entire span; and in region (ii) normal flow outboard of $r = -\mu\sin\psi$ and reverse flow inboard. Region (iii) is encountered only if $\mu > 1$. The aerodynamic coefficients were obtained using a rigid blade motion, and should properly be changed some to handle a blade with cantilever root restraint. However, the major effects of a cantilever root on the dynamics of the system are due to changes in ν and γ (both are increased, ν to 1.15 say and γ to about 5/3 the Lock number based on the rigid mode inertia). Since these are free parameters in the analysis this formulation of the problem should give reasonable results for all rotors.

This equation has been studied numerically in recent literature, primarily in the context of Floquet theory,[2] which must be used because the aerodynamic coefficients are periodic in ψ if $\mu \neq 0$. However, purely numerical solutions are not very satisfactory for obtaining an understanding of the physical characteristics of the system, or for formulating general design rules. An analytic solution for this equation in its general form would be difficult to obtain (if possible at all) and would be so complex as to be hardly better than the numerical solution. Time varying or nonlinear differential equations are characteristic features of helicopter dynamics and aerodynamics, primarily due to the rotation of the wing. The only solution procedure generally applicable to such problems is the numerical integration of the equations of motion. In particular cases, when there is some parameter which is either small or large, the techniques of perturbation theory may be used to obtain analytic solutions. Thus it is appropriate to apply the techniques to the study of rotor flapping stability. Perturbation theory has been well developed in recent years (e.g., Refs. 3 and 4), but has not yet found widespread application to rotary wing problems. This paper considers an example of such an application.

All the details of the mathematical analysis are not appropriate for this paper. The mathematical techniques are not very sophisticated actually; there are some tricks to be learned, but the standard ones work for most systems, including this one.[3,4] However the mathematics can be rather long and cumbersome, especially when the higher order solutions are sought. Furthermore it is not maintained that the differential equation studied is a true model of rotor dynamics; nonlinear aerodynamics and coupling with pitch and lag motions are certainly very important. The purpose of this paper is not to describe the mathematical details of perturbation techniques or to present a study of true flapping dynamics. Rather it is intended to demonstrate what information can be obtained by the perturbation techniques, and to explore the methods which are most useful for rotor dynamics, so helicopter engineers will be able to decide whether to use these techniques with more complicated or more realistic systems. Therefore only an outline of the method is presented, with primary attention to the results obtained. For more details of the analysis the reader is directed to Ref. 5.

For the flapping equation there are two parameters which may be used for perturbation quantities: the advance ratio μ and the Lock number γ. Then there are four cases to be considered: small and large μ, and small and large γ. The dynamic problem considered here is the question of rotor flapping stability. The stability of the motion is determined by the roots or eigenvalues of the system (there are two for this second order equation) and so most of the results will be concerned with the roots. The equation considered is linear; perturbation theory is used because the aerodynamic coefficients are time varying (specifically, periodic) for forward flight, i.e., when μ is greater than zero. Each of the four cases for this problem will be considered in turn below. First however, brief discussions will be given of the perturbation techniques used and the behavior expected of the eigenvalues of a periodic system.

Perturbation Techniques

Fundamental to perturbation theory is the existence of some parameter which is either very small or very large; for the moment represent the small parameter (or the inverse of the large parameter) by ϵ. In the present problem, it is desired to find the roots of the system, which means investigating a solution which is uniformly valid over long time periods. The appropriate perturbation technique is the method of multiple time scales. This method assumes that the behavior of the system may be investigated over several time scales, $\psi_n = \epsilon^n \psi$. The time scales ψ_n are all assumed to be of the same order; then for $\psi_1 = \epsilon \psi$ the actual time ψ must of order ϵ^{-1}, i.e. very large compared to the basic scale $\psi_0 = \psi$. The derivative with respect to ψ becomes then

$$\frac{d}{d\psi} = \frac{\partial}{\partial \psi_0} + \epsilon \frac{\partial}{\partial \psi_1} + \epsilon^2 \frac{\partial}{\partial \psi_2} + \cdots$$

so the use of these time scales amounts to an expansion of the time derivative as a series in ϵ. Next the dependent variable is expanded as a series in ϵ.

$$\beta = \beta_0 (\psi_0, \psi_1, \psi_2, \ldots) + \epsilon \beta_1 (\psi_0, \psi_1, \ldots) + \cdots$$

where the terms β_0, β_1, etc. are all assumed to be the same order, and depend on all the time scales. In addition, all free parameters (e.g., ν and γ for the small μ case) are also expanded as series in ϵ. These series for β, $d/d\psi$ and the free parameters are substituted into the equation of motion, and all terms of order ϵ^n are collected and separately equated to zero, giving the $o(\epsilon^n)$ equation. With the above expansion of $d/d\psi$, these equations are partial differential equations now. The requirement that all β_n be of the same order for the long time scale behavior of the motion is crucial to obtaining the solution of the partial differential equations. It leads, for certain values of the free parameters, to critical regions characterized typically by a reduction of the stability of the system. The method of multiple time scales is used for the small μ and small γ cases. Details of the method, and its use for these two cases, may be found in Refs. 3 and 5.

Often an equation of motion is such that in the limit $\epsilon = 0$ the order of the differential equation is reduced. The large γ and large μ cases are of this type; for example letting $\gamma \to \infty$ results in a first order equation (just the RHS of Eq. (1)), which is independent of γ. Such problems are called boundary layer problems, since they are characterized by narrow regions in which the solution changes greatly. The solution outside such regions may be found by use of a substitution of the form $\beta = \exp(\int^{\psi} p\, d\psi)$ followed by an expansion of p as a series in ϵ:

$$p = \frac{1}{\epsilon^n} p_{-n} + \cdots + p_0 + \epsilon p_1 + \cdots$$

This main solution is not valid in certain narrow transition regions or boundary layers. A basic part of this perturbation technique is methods to obtain solutions through the transition regions, so that it is possible to match one main solution to another on the other side of the transition region, or to boundary conditions at the base of the boundary layer. The matching procedure is so fundamental to the analysis of boundary-layer types of problems, that it gives the technique its name: the method of matched asymptotic expansions. Details of the method and its application may be found in Refs. 3, 4, and 5. Again, for stability problems the behavior of the solution over long time periods is of interest; the method of matched asymptotic expansions is used to construct such a solution, from which the eigenvalues of the system may be found.

The methods of perturbation theory are best described by example. Since the mathematics involved can be long, especially for higher order solutions, a detailed description of the procedures will not be given here. The reader is directed to Ref. 5 for the detailed

consideration of the rotor flapping equation. When first learning the techniques, the reader might want to consider simpler equations as examples, and these may be found in Refs. 3 and 4.

Periodic Systems

The root loci of a constant coefficient system typically exhibit behavior in which two roots start as complex conjugates, meet the real axis, and proceed in opposite directions along the real axis. The existence of periodic coefficients in the differential equations of motion generalizes this behavior so that it can occur at any $\mathrm{Im}\lambda = n/\mathrm{rev}$ or $n+1/2/\mathrm{rev}$, not just at $\mathrm{Im}\lambda = 0$. The property of the solution that allows this behavior is the fact that the eigenvectors are themselves periodic (instead of constant as for a constant coefficient system). The analysis that demonstrates that periodic systems show this behavior is called Floquet theory. Thus the following behavior of root loci is characteristic of periodic systems. If the parameter being varied, for example the advance ratio μ, is such that at $\mu = 0$ the system is not periodic, then the roots start out as complex conjugates. As μ increases, the periodicity of the system increases, and the roots move toward n/rev (or $n + 1/2/\mathrm{rev}$) lines (remaining complex conjugate pairs though). At some critical μ the loci reach $\mathrm{Im}\lambda = n/\mathrm{rev}$, and then for still larger μ the frequency remains fixed at n/rev while the real part of one root is decreased and that of the other is increased. The root being destabilized usually crosses into the RHP for some μ, indicating the system has become unstable because of the influence of the periodic coefficients.

The Small μ Case

The small parameter in this case is the advance ratio μ. Setting $\mu = 0$ gives the hover case; the time variation of the aerodynamic coefficients is removed and the roots are easily obtained. To order μ^2 the reverse flow region may be ignored, and the expressions for $M_{\dot\beta}$, M_β, and M_θ in region (i) may be used for all ψ. To obtain the roots it is necessary to find a solution valid over long time periods; thus the appropriate perturbation technique is the method of multiple time scales. This method involves considering the behavior of β when ψ is of order 1, of order μ^{-1}, of order μ^{-2}, etc. β is expanded as a series in μ:

$$\beta = \beta_0 + \mu\beta_1 + \mu^2\beta_2 + \ldots$$

and the method yields a solution uniformly valid for all ψ. ν and γ are also expanded in μ:

$$\gamma = \gamma_0 + \mu\gamma_1 + \mu^2\gamma_2 + \ldots$$

$$\nu = \nu_0 + \mu\nu_1 + \mu^2\nu_2 + \ldots$$

This is done because it is the characteristic of systems with periodic coefficients that for certain values of ν_0 and γ_0 there are stability degradation regions described by boundaries in ν_1 and γ_1 (or ν_2 and γ_2, etc.). The case $K_R = 0$ will be considered first.

Order 1 Results

To order 1 the roots are the hover roots, given by

$$\lambda_0 = -\frac{\gamma_0}{16} + i\sqrt{\nu_0^2 + \frac{\gamma_0}{8}K_P - \left(\frac{\gamma_0}{16}\right)^2} \qquad (2)$$

and its conjugate. The variation of these roots with γ for $\nu = 1$ and several K_P is shown in Fig. 1 (the $\mu = 0$ loci).

Order μ Results

To order μ the roots for most ν_0 and γ_0 are still the hover roots:

$$\lambda = \lambda_0 + \mu\lambda_1 = -\frac{\gamma}{16} + i\sqrt{\nu^2 + \frac{\gamma}{8}K_P - \left(\frac{\gamma}{16}\right)^2} \qquad (3)$$

To this order there is no effect of the periodic coefficients. The exception is when $\mathrm{Im}\lambda_0 = 1/2$ (the frequency of the hover root is near $1/2/\mathrm{rev}$) i.e. ν_0 and γ_0 such that

$$\nu_0^2 + \frac{\gamma_0}{8}K_P - \left(\frac{\gamma_0}{16}\right)^2 = \frac{1}{4} \qquad (4)$$

There is then a critical region, with a boundary described by the following equation.

$$2\nu_0\nu_1 = \left(\frac{\gamma_0}{8} - 2K_P\right)\frac{\gamma_1}{16} \pm \frac{\gamma_0}{24}\sqrt{1 + \left(\frac{\gamma_0}{8} - 4K_P\right)^2} \qquad (5)$$

This equation describes a narrow band, of width $O(\mu)$, about $\mathrm{Im}\lambda_0 = 1/2$ (which by Eq. (4) may be considered a line of ν as a function of γ). Outside the critical region there is an $O(\mu)$ change in the frequency while the real part of the root is unchanged from the hover root. Inside the critical region the frequency is fixed at $1/2/\mathrm{rev}$ while there is an $O(\mu)$ change in the damping. This behavior is illustrated by the $\mu = 0.1$ loci in Fig. 1. The maximum stability change occurs at $\nu_1 = \gamma_1 = 0$ (i.e. when ν and γ are such that the frequency of the hover root is exactly $1/2/\mathrm{rev}$), where the root is

$$\lambda = \frac{1}{2} - \frac{\gamma}{16} \pm \mu\frac{\gamma_0}{24}\sqrt{1 + \left(\frac{\gamma_0}{8} - 4K_P\right)^2} \qquad (6)$$

The critical region is a region of stability degradation, not of instability; the maximum reduction (and enhancement) in the damping is

$$\left(\frac{\Delta\lambda}{\mathrm{Re}\lambda}\right)_{max} = \mu\frac{\gamma_0}{24}\sqrt{1+\left(\frac{\gamma_0}{8}-4K_P\right)^2}\Big/\frac{\gamma_0}{16}$$

$$= \frac{2}{3}\mu\sqrt{1+\left(\frac{\gamma_0}{8}-4K_P\right)^2}$$

$$= \frac{4}{3}\mu\sqrt{\nu_0^2 - \frac{\gamma_0}{8}K_P + 4K_P^2} \qquad (7)$$

which is an $O(\mu)$ small reduction. The system remains stable because of the large hover damping. Fig. 1 shows typical root loci for varying γ, with $\mu = 0$ and $\mu = 0.1$. The point D on the hover locus ($K_P = 1$) is where the locus crosses $\mathrm{Im}\lambda = 1/2$. As μ increases, since this point is at the center of the critical region it receives the maximum stability change, and so is pulled out to the point B. In terms of the γ locus, as γ increases and the hover locus nears $\mathrm{Im}\lambda = 1/2$, the root has an $O(\mu)$ change in the frequency, pulling the locus toward $\mathrm{Im}\lambda = 1/2$. When the locus crosses into the critical region the frequency has just reached 1/2/rev, and the root locus is at the point A. For still larger γ the frequency remains fixed while the real part of one root decreases and that of the other increases. When γ reaches the value for which the hover root has a frequency of 1/2/rev, the locus is at the center of the critical region; there the roots have their maximum stability change (which is $O(\mu)$) so the locus is at the point B. As γ increases more, the locus moves toward the other boundary of the critical region. The locus reaches that boundary at the point C, and for still larger γ the frequency is no longer fixed at 1/2/rev; rather the real part of the root is the same as the hover value, while there is an $O(\mu)$ change in the frequency which decreases in size as γ increases. For still larger γ the locus is again identical (to order μ) to the hover locus.

Figure 2 shows typical root loci for fixed γ and varying μ. The circle the locus starts from is the γ locus for hover ($\mu = 0$) and the appropriate K_P. The γ for each locus may be found from $\mathrm{Re}\lambda$ at $\mu = 0$, since for the hover root $\mathrm{Re}\lambda = -\gamma/16$. As μ increases from zero, for the roots near $\mathrm{Im}\lambda = 1/2$ there is an $O(\mu)$ change in the frequency pulling the root toward $\mathrm{Im}\lambda = 1/2$; while the damping remains fixed at the hover value. The locus reaches $\mathrm{Im}\lambda = 1/2$ for a corner μ which corresponds to the boundary of the critical region. For larger μ, frequency remains fixed at 1/2/rev while one branch of the locus moves to the left (decreased stability) and the other to the right (increased stability). This behavior of the μ loci is characteristic of roots of a system with periodic coefficients.

Order μ^2 Results

To order μ^2 the roots for most ν_0 and γ_0 are

$$\lambda = -\frac{\gamma}{16} + i\left\{\nu^2 + (1+\mu^2)\frac{\gamma}{8}K_P - \left(\frac{\gamma}{16}\right)^2\left[1 - \mu^2\frac{8}{9}\frac{\nu^2 - \frac{\gamma}{8}K_P + 4K_P^2}{\left(\frac{\gamma}{16}\right)^2 - \nu^2 - \frac{\gamma}{8}K_P + \frac{1}{4}}\right]\right\}^{\frac{1}{2}} \qquad (8)$$

and its conjugate. Thus away from $\mathrm{Im}\lambda = 1/2$ or 1 the roots are just the hover roots with an $O(\mu^2)$ change in the frequency. There are two effects of μ; the first corrects the term $\gamma/8\,K_P$ in the hover frequency to properly account for the average of $K_P M_\theta$. The second effect, that in the last term of the frequency, is entirely due to the periodic aerodynamic coefficients; this is the first effect of the periodic coefficients seen in the analysis, except for the critical region near $\mathrm{Im}\lambda = 1/2$. Typical root loci for varying μ are shown in Fig. 2. These are the loci that are not near $\mathrm{Im}\lambda = 1/2$ or 1; the frequency change is small even at $\mu = 0.5$. Eq. 8 may also be used for the branches of the root loci on the real axis when the quantity under the square root sign is negative (i.e., for γ large enough). There are two real roots then, the $(+i)$ in the frequency becoming (± 1). A point on the locus of special interest is where one branch of the locus on the real axis crosses into the RHP, i.e., becomes unstable (as in Fig. 1). The criterion for this divergence boundary is $\lambda = 0$, or to order μ^2:

$$(1+\mu^2)\frac{\gamma}{8}K_P = -\nu^2\left[1 + \mu^2\frac{16}{9}\frac{\left(\frac{\gamma}{16}\right)^2 + \frac{\nu^2}{2}}{\left(\frac{\gamma}{16}\right)^2 + \frac{1}{4}}\right] \qquad (9)$$

The effect of μ on the RHS (due to the periodic coefficients) dominates that on the LHS (due to the average of $K_P M_\theta$) for all values of γ and ν. Thus the critical value of negative K_P, beyond which the locus lies in the RHP, is actually increased by increasing μ. The criterion from the hover case is conservative then; this is the opposite of the conclusion that would have been reached from a consideration of the averaged coefficients only.

To order μ^2 there is a critical region when $\mathrm{Im}\lambda_0 = 1$, i.e., when

$$\nu_0^2 + \frac{\gamma_0}{8}K_P - \left(\frac{\gamma_0}{16}\right)^2 = 1 \qquad (10)$$

The behavior of the loci near the critical region is similar to that near $\mathrm{Im}\lambda_0 = 1/2$, except that now changes are $O(\mu^2)$, not $O(\mu)$. The boundary of the critical region is described by a relation between ν_2 and γ_2 with $\nu_1 = \gamma_1 = 0$; the critical region is thus

a narrow band, of width $O(\mu^2)$, about $\mathrm{Im}\lambda = 1$. Inside the critical region the frequency is fixed at $\mathrm{Im}\lambda = 1$ with an $O(\mu^2)$ change in the damping. The maximum reduction (or enhancement) of the damping is

$$\left(\frac{\Delta\lambda}{\mathrm{Re}\lambda}\right)_{max} = \frac{\mu^2}{2}\left\{\left[1 + \frac{\gamma_0}{9}\left(\frac{\gamma_0}{16} - 2K_P\right)\right]^2 + \left[K_P - \frac{\gamma_0}{9}\left(\frac{\gamma_0}{16} - 2K_P\right)^2\right]^2\right\}^{\frac{1}{2}} \qquad (11)$$

which is an $O(\mu^2)$ small reduction in the large hover damping. Figs. 1 and 2 show typical root loci near $\mathrm{Im}\lambda = 1$ for varying γ and μ.

Flap Rate Feedback

The use of flap rate feedback, $K_R \neq 0$, does not change the behavior of the solution quantitatively. The hover root becomes

$$\lambda_0 = -\frac{\gamma_0}{16}\left(1 + K_R\right) + i\left\{\nu_0^2 + \frac{\gamma_0}{8}K_P - \left[\frac{\gamma_0}{16}\left(1 + K_R\right)\right]^2\right\}^{\frac{1}{2}} \qquad (12)$$

and there are critical regions about $\mathrm{Im}\lambda_0 = 1/2$ and 1 again. The critical region boundaries and stability degradation depend on K_R now. It is necessary that $K_R > -1$ for the hover root to be stable, but $K_R > 0$ will be the usual case anyway.

$\gamma - \mu$ Plane

The results of the small μ analysis may be used to plot lines of constant $\mathrm{Re}\lambda$ and $\mathrm{Im}\lambda$ on the γ-μ plane. Typical results are shown in Figs. 3, 4, and 5 for $\nu = 1.0$ and $K_P = 0$, 0.1, and -0.1, respectively. The critical regions appear in the γ-μ plane as regions in which $\mathrm{Im}\lambda$ is constant (at 1/2/rev or 1/rev); they are indicated in the figures by the circled values of $\mathrm{Im}\lambda$ (the region where $\mathrm{Im}\lambda = 0$ is where there are two real roots, not a critical region). These figures are interpreted as follows. A horizontal line is a line of constant γ, and so as μ varies it gives the corresponding values of $\mathrm{Re}\lambda$ and $\mathrm{Im}\lambda$ just as a μ root locus does. Similarly a vertical line is a constant μ line, and so gives λ as a function of γ just as a γ root locus does. For example, consider a horizontal line in Fig. 3 ($K_P = 0$) with $\gamma = 8$, i.e., $\gamma/16 = 0.5$. As μ increases, the line remains parallel to the $\mathrm{Re}\lambda$ = constant lines so $\mathrm{Re}\lambda$ remains fixed at the hover value. The $\mathrm{Im}\lambda = 1/2$ region comes closer to the horizontal line as μ increases, which means that $\mathrm{Im}\lambda$ moves toward 1/2/rev. Eventually the constant γ line crosses into the $\mathrm{Im}\lambda = 1/2$ region; then $\mathrm{Im}\lambda$ is fixed at 1/2/rev while for each point in the region there are two values of $\mathrm{Re}\lambda$, giving the damping for the two branches (one more and one less stable than the hover root). This behavior is just that seen already in the μ loci (Fig. 2). Figs. 3, 4, and 5 may be compared with similar ones in Ref. 2, which were constructed from numerical calculations; on the basis of this comparison, the $O(\mu^2)$ analytic results are quite accurate up to $\mu = 0.5$ or so. There is some discrepancy between the results for the $\mathrm{Im}\lambda = 1$ region however, particularly with $K_P = -0.1$, although the change in scale (Ref. 2 shows results out to $\mu = 2.5$) exaggerates the difference. For ν exactly 1 the analytic results indicate no critical region if $K_P < 0$; but only a slightly larger (for example $\nu = 1.01$) is necessary to get a sizable critical region with $K_P = -0.1$ (see Fig. 5). The analytic results show the $\nu = 1$ case is a very sensitive one for small γ and small K_P, and it is unlikely that a numerical calculation could treat the case accurately. Of course an actual rotor will always have ν at least slightly greater than 1, so the numerical calculations are probably reliable then; furthermore, the discrepancy may also be an indication that for very small γ the analytic results (to order μ^2) are not valid out to as large a μ as they are for more reasonable γ. In any case this discussion illustrates the kinds of problems that may be hidden in a purely numerical solution; they can only be found and studied by analytic procedures (which at least tell where to look for problems).

The Small γ Case

The small parameter in this case is the Lock number γ. Setting $\gamma = 0$ removes all the aerodynamic terms, and the roots are $\lambda = \pm i\nu$ for all μ. The method of multiple time scales is used to obtain solutions uniformly valid for all ψ. The time scales considered are of order 1, of order γ^{-1}, etc. β is expanded as a series in γ ($\beta = \beta_0 + \gamma\beta_1 + \ldots$) and so is ν ($\nu = \nu_0 + \gamma\nu_1 + \ldots$). The advance ratio μ is not small now, and the reverse flow region must be considered.

Order γ Results

If $\nu_0 \neq n/2$ for any integer n (i.e. $\mathrm{Im}\lambda_0$ not equal to a multiple of 1/2/rev) the root to $O(\gamma)$ is

$$\lambda = \frac{\gamma}{2}\left(M_{\dot\beta}^0 - K_R M_\theta^0\right) + i\nu\left[1 - \frac{\gamma}{2\nu^2}\left(M_\beta^0 - K_P M_\theta^0\right)\right] \qquad (13)$$

where $M_{\dot\beta}^0$, M_β^0, and M_θ^0 are the averages of the aerodynamic coefficients around the azimuth. For the coefficients considered here, $M_{\dot\beta}^0 = 0$ for all μ. Flap rate feedback only effects (to order γ) the damping; the real part of may be written

$$\mathrm{Re}\lambda = \left(\frac{\gamma}{2}\right) M_{\dot\beta}^0 \left(1 + \frac{K_R}{-M_{\dot\beta}^0/M_\theta^0}\right) \qquad (14)$$

The ratio $-M_{\dot\beta}^0/M_\theta^0$ determines the relative effect of K_R; this ratio is shown in Fig. 6 as a function of μ.

This parameter is a positive number, which varies little with μ (from 1 at $\mu = 0$ to 1/2 at $\mu = \infty$, with most of the change below $\mu = 1$). The negative of this ratio gives a critical K_R, since it is necessary that $K_R > K_{R_{crit}} = M^0_{\dot\beta}/M^0_\theta$ in order that the system be stable for small γ (to $O(\gamma)$ and with $\nu_0 \neq n/2$). For $K_R = 0$ the root is

$$\lambda = -\frac{\gamma}{16}\left(-8M^0_{\dot\beta}\right) + i\nu\left[1 + \frac{\gamma}{16}\frac{K_P}{\nu^2}\left(8M^0_\theta\right)\right] \quad (15)$$

The aerodynamic coefficients $-8M^0_{\dot\beta}$ and $8M^0_\theta$ are always positive; they have the value 1 for $\mu = 0$ and are asymptotic to $(8/3\pi)\mu$ and $(16/3\pi)\mu$, respectively, for large μ; these coefficients are shown in Fig. 7.

The root loci for varying γ and varying μ are shown in Fig. 8 for $K_P = 1$, $K_R = 0$, and $\nu = 1$; the locus for $K_P = -1$ is obtained by reflecting this locus about the $\mathrm{Im}\lambda = \nu$ line. The locus for $K_P = 0$ is difficult to plot since $\mathrm{Im}\lambda = \nu$ for all γ and μ (to order γ); it may be visualized by projecting the $K_P = 1$ loci onto the line $\mathrm{Im}\lambda = \nu$. These loci should be compared with the small γ portions of the curves in Fig. 1, which are for small μ. In Fig. 8, the γ locus for a given μ starts out at $\lambda = i\nu$ always, and is a straight line with slope

$$\frac{\partial \mathrm{Im}\lambda}{\partial \mathrm{Re}\lambda} = -\frac{K_P}{\nu}\frac{1}{-M^0_{\dot\beta}/M^0_\theta}$$

which varies from $-K_P/\nu$ to $-2K_P/\nu$ for μ from 0 to ∞ (see Fig. 6 for $-M^0_{\dot\beta}/M^0_\theta$). The step size on the γ locus, for a unit change in $\gamma/16$, is

$$\sqrt{\left(8M^0_{\dot\beta}\right)^2 + \left(K_P/\nu\right)^2\left(8M^0_\theta\right)^2},$$

which varies from

$$\sqrt{1 + \left(K_P/\nu\right)^2}$$

to

$$\frac{9}{8}\sqrt{1 + \frac{25}{9}\left(K_P/\nu\right)^2}$$

to

$$\frac{8}{3\pi}\mu\sqrt{1 + 4\left(K_P/\nu\right)^2}$$

for μ from 0 to 1 to ∞, respectively. The μ locus for a given γ starts out virtually from the $\mu = 0$ line, and is asymptotic to the $\mu = \infty$ line, with the step size on the locus for a unit change in μ increasing as μ increases. For reasonable μ the locus does not vary much from the small μ results. An $O(\gamma)$ analysis can only obtain the slope of the γ locus at $\gamma = 0$, so the locus is a straight line, as found above; to find the curvature effect it is necessary to go to order γ^2. The significance of the curvature (order γ^2) may be judged from a comparison of the γ loci of Fig. 8 (all μ, small γ) and Fig. 1 (small μ, all γ); on this basis the small γ results should be limited to $\gamma/16$ less than 0.2. On the basis of neglect of the curvature effects alone the results might be accepted to higher γ, but the $O(\gamma)$ results will also be limited by the effects of the critical region, which will be examined next.

The discussion of the $O(\gamma)$ analysis has so far only been concerned with the basic roots, meaning the roots away from the influence of a critical region. In the small γ case, the criterion for being away from a critical region is that $\nu_0 \neq (n/2)$ for any integer n; this may be written

$$\nu \neq \left(\frac{n}{2}\right) + O\left(\frac{\gamma}{16}\right)$$

i.e., the rotating natural frequency may not be a distance of order $\gamma/16$ from n/2/rev. Since ν is almost always just above 1/rev this criterion is seldom fulfilled, and the critical regions may be expected to dominate the root loci behavior for small γ. Furthermore, if K_P is large enough positive or negative, the basic locus will also cross $\mathrm{Im}\lambda = 3/2$ or 1/2 for $\gamma/16$ still small (see Fig. 8), so these critical regions may affect the loci even if the $\mathrm{Im}\lambda = 1$ region does not.

If $\nu_0 = n/2$ for some integer n, there arise critical regions, with behavior of the root loci similar to that encountered already in the small μ case. The case $K_R = 0$ will be considered first. The critical region boundary is given by

$$\nu_1 = -\frac{K_P}{2\nu}M^0_\theta \pm \frac{1}{2\nu_0}\sqrt{\left|M^n_{\dot\beta} - i\nu_0 M^n_{\dot\beta}\right|^2 + K_P{}^2\left|M^n_\theta\right|^2} \quad (16)$$

where

$$M^n_\beta = \frac{1}{2\pi}\int_0^{2\pi} M_\beta e^{-in\psi}\,d\psi,$$

and similarly for $M^n_{\dot\beta}$ and M^n_θ (i.e., the nth harmonic in a complex Fourier series representation of the

aerodynamic coefficients). This equation describes a band of width $O(\gamma)$ about $\mathrm{Im}\lambda = n/2$. The maximum stability change occurs at $\nu_I = -(K_P/2\nu_0)\, M_\theta^0$, that is at the center of the critical region, where the basic root (Eq. 15) would cross $\mathrm{Im}\lambda = \nu_0 = n/2$. There the root is

$$\lambda = i\nu_0 + \frac{\gamma}{2}\left(M_\beta^0 \pm \frac{1}{\nu_0}\sqrt{\left|M_\beta^n - i\nu_0 M_\beta^n\right|^2 + K_P^2\left|M_\theta^n\right|^2}\right) \tag{17}$$

Outside the critical region there is an order γ change in the frequency of the basic root with no change in the damping. Inside the critical region the frequency is fixed at n/2/rev while there is an order γ change in the damping. The damping of the basic root is itself $O(\gamma)$ however, so in contrast to the small μ case, the critical region can here lead to actual instability, not just stability degradation.

The root loci for small γ show the behavior characteristic of periodic systems, and familiar from the discussion of the loci for the small μ case. For some μ or γ the locus will cross into the critical region. The maximum stability change inside the critical region occurs at the center, which is where the basic root locus (e.g., as shown in Fig. 8) would have crossed $\mathrm{Im}\lambda = n/2$. Whether the center is ever reached depends on the parameters involved (K_P, ν, γ, μ). For the $O(\gamma)$ analysis, the locus has a slope proportional to K_P, so for $|K_P|$ not too small the locus will probably cross some $\mathrm{Im}\lambda = n/2$ line with $\gamma/16$ still small (e.g., in Fig. 8 where $K_P = 1$, the loci cross the $\mathrm{Im}\lambda = 3/2$ line). If $K_P = 0$ however, there is no $O(\gamma)$ change in the frequency, so $\mathrm{Im}\lambda = \nu$ for all μ and γ. Then the locus will never reach the center of the critical region (cross $\mathrm{Im}\lambda = n/2$) unless $\nu = n/2$, in which case the locus is always at the center. More generally, if $|K_P|$ is very small, the locus will not cross $\mathrm{Im}\lambda = n/2$ until $\gamma/16$ is so large as to be outside the range of the order γ analysis. An $O(\gamma^2)$ analysis would change significantly the conclusions about whether the center of the critical region is reached under certain conditions, particularly for small $|K_P|$ when the $O(\gamma^2)$ change in the frequency is more important than the $O(\gamma)$ change. For example, Fig. 1 indicates that with ν slightly greater than 1 the γ locus (for small μ) would never cross $\mathrm{Im}\lambda = 3/2$ for $K_P = 1$ while it would always cross $\mathrm{Im}\lambda = 1$ for $K_P = 0$, just the opposite of the conclusions indicated by the $O(\gamma)$ results (Fig. 8). In any case, since the maximum stability change occurs at the center of the critical region, it is useful to examine it as a worst possible case, which may perhaps be approached but never reached for certain values of ν and K_P.

Considering the μ root locus again, the maximum change in the damping from the value of the basic root is given by the real part of Eq. 17. The contribution from the basic root damping, $(\gamma/2)M_\beta^0$, is always negative (Fig. 7); as for the small μ case it is $O(\gamma)$, but here that means the basic damping is small. In fact it is the same order as the critical region contribution, so the destabilized root may be actually unstable, rather than just a small perturbation from the basic damping as for the small μ case. The behavior of the locus depends on the relative effects of M_β^0 and the nth harmonics of the aerodynamic coefficients under the square root in Eq. (17). For most cases the critical region effect dominates, so that as μ increases it eventually reaches a critical value, at which point (for the case of maximum stability change) one root crosses into the RHP, i.e., becomes unstable. From Eq. 17, it follows that increasing K_P^2 (K_P either positive or negative) always increases the effect of the critical region, which means decreasing the critical μ for which the root becomes unstable. Thus the critical μ is a function of $|K_P|$, for each of the critical regions; this function may be found from Eq. (17) by setting $\mathrm{Re}\lambda = 0$ (the requirement for crossing the $\mathrm{Im}\lambda$ axis). Since the aerodynamic coefficients are rather complex functions of μ, it is more convenient to find the critical $|K_P|$ as a function of μ:

$$|K_P|_{\mathrm{crit}} = \sqrt{\frac{\left(\nu_0 M_\beta^0\right)^2 - \left|M_\beta^n - i\nu_0 M_\beta^n\right|^2}{\left|M_\theta^n\right|^2}} \tag{18}$$

This may be regarded as a maximum $|K_P|$ for a given μ; for larger $|K_P|$ the locus is in the RHP at that μ. These boundaries of $|K_P|$ vs. μ are shown in Fig. 9 for $\mathrm{Im}\lambda = 1/2$, 1, and 3/2. With the exception of the roots near $\mathrm{Im}\lambda = 1/2$ with μ above 0.5 or so, Fig. 9 shows the criterion on $|K_P|$ is not very stringent. Fig. 9 shows also that near $\mathrm{Im}\lambda = 1$ the roots are always stable, regardless of μ, if $|K_P| < \sqrt{2}$; the loci may be expected to be near $\mathrm{Im}\lambda = 1$ for zero or small K_P. In terms of the μ locus, this means that as μ increases the locus does not cross into the RHP. Just after the locus crosses the critical region boundary, the effect of the critical region is seen and one branch moves to the right and the other to the left (as do the loci in Fig. 2). As μ increases further however, the damping of the basic root (which is always stable, and increases with μ) eventually dominates the effect of the critical region, and the root which was becoming less stable turns around before reaching the RHP. So for still larger μ both branches of the locus will be moving to the left, i.e. becoming more stable as μ increases. For the root loci near $\mathrm{Im}\lambda = 1/2$ or 3/2, the effect of the critical region remains dominant, and so one root eventually crosses into the RHP as μ is increased. The critical μ is considerably lower for $\mathrm{Im}\lambda = 1/2$ than for $\mathrm{Im}\lambda = 3/2$. This points out an undesirable feature of negative pitch flap coupling, $K_P < 0$; not so much that it reduces the critical μ, but rather that it moves the basic root nearer to $\mathrm{Im}\lambda = 1/2$.

The use of flap rate feedback, $K_R \neq 0$, results in no qualitative changes in the behavior of the loci. K_R is however a useful design parameter; it may be used for example to raise the critical μ or $|K_P|$.

Evaluation of the Order γ Results

Numerical calculations were made of the μ root loci for moderate and small values of γ. On the basis of a comparison of the numerical and analytic results, it is concluded that the small γ analysis to order γ is useful only for truly small γ, e.g., $\gamma = 2$ or 3 ($\gamma/16 = 0.2$ or so). Problems are encountered with both the basic roots and the effects of the critical region. The basic root to order γ neglects the curvature of the γ locus, which is especially important for zero or small K_P, since then the change of $\mathrm{Im}\lambda$ for small γ is due more to $O(\gamma^2)$ terms than to the $O(\gamma)$ term. The damping of basic root is $O(\gamma)$ always, no matter what order the analysis is carried too; for example the $O(\mu^2)$ results give $\mathrm{Re}\lambda = -\gamma/16$ for all γ. However while basic damping is $O(\gamma)$, the contribution to the damping due to the critical region will have terms that are $O(\gamma^2)$. Thus for large enough γ the conclusions in the discussion above of the effects of the critical region on the μ root loci will not be valid, since they depend on the basic and critical region damping being of the same order in γ. In particular, the behavior of the locus in which the root being destabilized by the critical region turns around and becomes more stable due to the eventual dominance of the basic damping is not possible except for very small γ, for which $O(\gamma^2)$ effects are in fact negligible. Indeed, it was found in the numerical calculations that with $\gamma = 6$ ($\gamma/16 = 0.375$, which is not very small), ν near 1, and K_P zero or small so the root is near 1/rev, that the μ locus does not turn around but rather eventually crosses into the RHP. The stability boundaries given in Fig. 9 are only valid then for truly small values of $\gamma/16$.

Order γ^2 Results

To order γ^2 the basic root, valid for $\nu_0 \neq n/2$, is (with $K_R = 0$)

$$\lambda = \frac{\gamma}{2} M_{\dot\beta}^0 + i\nu \left\{ 1 + \frac{\gamma}{2\nu^2} K_P M_\theta^0 - \frac{\gamma^2}{8\nu^2} \left[M_{\dot\beta}^{0\,2} + \left(K_P/\nu\right)^2 M_\theta^{0\,2} \right] \right\} \qquad (19)$$

As reported above, there is no $O(\gamma^2)$ change in $\mathrm{Re}\lambda$, and the $O(\gamma^2)$ change in the frequency is dominant for small K_P, indeed for $K_P = 0$ the only change in $\mathrm{Im}\lambda$ is $O(\gamma^2)$. The $O(\gamma^2)$ results would significantly alter the plots of the basic root loci shown in Fig. 8.

The Large γ Case

The small parameter in this case is the inverse of the Lock number, γ^{-1}. For γ very large, the aerodynamics dominate the system. For $\gamma = \infty$ the inertia and centrifugal spring terms are negligible, leaving a first-order system that does not depend on γ. This system gives one real root, which is independent of and valid for $\gamma = \infty$. The reduction of order of the equation at $\gamma = \infty$ is a characteristic of a boundary-layer type of problem. This characteristic means that one of the roots goes to $-\infty$ as γ goes to ∞. The two roots may be found by use of the following substitution.

$$\beta = \exp \int^{\psi} \gamma\, p_{-1} + p_0 + \frac{1}{\gamma} p_{-1} + \ldots d\psi$$

This substitution gives two solutions, from which the two roots are obtained as (for $K_R = 0$):

$$\lambda_1 = -K_P \frac{1}{2\pi} \int_0^{2\pi} \frac{M_\theta}{-M_{\dot\beta}} d\psi + \frac{1}{\gamma} \frac{1}{2\pi} \int_0^{2\pi} \frac{\nu^2 - \frac{d}{d\psi}\left(\frac{M_\beta - K_P M_\theta}{M_{\dot\beta}}\right) + \left(\frac{M_\beta - K_P M_\theta}{M_{\dot\beta}}\right)^2}{M_{\dot\beta}} d\psi + O\left(\gamma^{-2}\right) \qquad (20)$$

$$\lambda_2 = \gamma \frac{1}{2\pi} \int_0^{2\pi} M_{\dot\beta}\, d\psi + K_P \frac{1}{2\pi} \int_0^{2\pi} \frac{M_\theta}{-M_{\dot\beta}} d\psi + O\left(\gamma^{-1}\right) \qquad (21)$$

Thus there are two real roots, one (λ_2) approaching $-\infty$ as γ increases to ∞ ($M_{\dot\beta}$ is negative), and the other (λ_1) approaching a constant. This behavior of the γ root loci is expected from the small μ results; Fig. 1 shows that for large enough γ the locus is on the real axis, i.e. there are two real roots, one approaching $-\infty$ and the other $-K_P$ for $\gamma \to \infty$. To lowest order λ_1 does not depend on γ, because it represents the balance of the aerodynamic damping and the aerodynamic spring only. The value of $\lambda_1/(-K_P)$ for varying μ, and $\gamma = \infty$, is shown in Fig. 10; the movement shown takes place entirely on the real axis in the λ plane. As for the small μ case (Fig. 1) the root on the real axis is in the LHP if $K_P > 0$ and in the RHP – unstable – if $K_P < 0$. The value of $\lambda_1/(-K_P)$ varies from 1 to 7/8 for $\mu = 0$ to ∞, with most of the change between $\mu = 0.5$ and $\mu = 1$; thus there is little variation of the root with μ (to order 1 in γ). The size of the $O(\gamma^{-1})$ term in λ_1 is indicated by the result for $\mu = 0$, which is easily obtained (since the aerodynamic coefficients are constant then) as

$$\lambda_1 = -K_P - \frac{1}{\gamma/16} \frac{\nu^2 + K_P^2}{2} + O\left(\gamma^{-2}\right)$$

To lowest order λ_2 is $-(\gamma/16)\,2\left(-8\,M_{\dot\beta}^{0}\right)$. The aerodynamic coefficient $-8\,M_{\dot\beta}^{0}$ is given in Fig. 7. For $\mu \leq 1$ it has the value $-8\,M_{\dot\beta}^{0} = 1 + \mu^2/8$; for large μ it is asymptotic to $(8/3\pi)\mu^3$. This root becomes increasingly negative as γ increases, and also as μ increases. The order 1 term in λ_2 is the negative of the lowest order term in λ_1; thus the behavior of this term is also given by Fig. 10.

The solution for the roots is not valid if $M_{\dot\beta} = 0$ for any ψ. When $M_{\dot\beta}$ is small, the assumptions made about the order of terms in deriving the solutions are violated; this may be inferred from the expressions obtained for the roots by the continual appearance of $M_{\dot\beta}$ in the denominator of the integrands (Eqs. (20 and (21). There is a narrow transition region, of width $O(\gamma^{-2/3})$, about any points where $M_{\dot\beta} = 0$, i.e., where the damping goes through zero. As it happens, however, $M_{\dot\beta}(\psi, \mu)$ is a negative quantity which never reaches zero. Thus for $K_R = 0$ there are no transition regions or boundary layers, and the solutions obtained from the substitution for β are uniformly valid over the entire azimuth.

Flap Rate Feedback

When $K_R = 0$, there are no boundary layers or transition regions because $M_{\dot\beta} < 0$ always. With flap rate feedback, $K_R \neq 0$, the same expressions for the main solutions for β are obtained as for $K_R = 0$, except that $M_{\dot\beta}$ is replaced by $M_{\dot\beta} - K_R M_\theta$. The aerodynamic coefficient $-(M_{\dot\beta} - K_R M_\theta)$ can become negative over regions of the disk for certain combinations of μ and K_R; that is, there may be negative damping over part of the azimuth range. When such regions of negative damping exist it means there must be transition regions about the points where the damping goes through zero. Since Eqs. (20) and (21) for λ_1 and λ_2 were derived on the basis of no transition regions, these expressions for the roots (with $M_{\dot\beta}$ replaced by $M_{\dot\beta} - K_R M_\theta$) are not valid when there is negative damping over any part of the disk.

The criterion for the existence of transition regions is that there be negative damping on some portion of the disk, i.e., $-(M_{\dot\beta} - K_R M_\theta) < 0$. $M_{\dot\beta}$ is always negative; M_θ is usually positive, but may be negative on the retreating side for large enough μ. If K_R is too large positive, the negative values of M_θ on the retreating side eventually dominate $M_{\dot\beta}$ as μ is increased, so there will be negative damping on the retreating side; if K_R is too large negative, $K_R M_\theta$ eventually dominates $M_{\dot\beta}$ on the advancing side and there will be negative damping there if μ is large enough. Quantitative values of maximum and minimum K_R as a function of μ are given in Fig. 11. For the cases with negative damping there will be transition regions (of width $O(\gamma^{-2/3})$) near where $M_{\dot\beta} - K_R M_\theta = 0$, which greatly complicates the analysis. For these cases it is also expected that there will be other problems, including numerical computation problems, physical control problems, and large flapping amplitudes. Thus while a region of negative damping does not necessarily mean there is a flapping instability, it does mean that there are many problems – analytical, computational, and physical – so requiring $-(M_{\dot\beta} - K_R M_\theta) > 0$ is a reasonable design criterion. This criterion provides a maximum and minimum K_R for a given μ. The limits of K_R from this rue are much easier to obtain than actual stability boundaries; and Fig. 11 shows that although conservative, it is not a serious restriction for μ less than 1 or 2. For large μ it is a serious limitation, indicating that M_θ (flap moment due to blade pitch) is not very good for flapping rate feedback then. Although the derivation of this rule has been based on the large γ case, the criterion of no negative damping has nothing to do with γ, and so should be a reasonable criterion for all γ. Indeed the criterion $K_R > -1$ for $\mu = 0$ is the same as from the small μ case, where it is a true stability criterion, and valid for all γ.

The Large μ Case

The small parameter for this case is the inverse of the advance ratio, μ^{-1}. For μ very large, the aerodynamics again dominate the system. However, for $K_R = 0$ the damping is $O(\mu)$ while the aerodynamic spring is $O(\mu^2)$, with the result that at $\mu \to \infty$ the aerodynamic spring must be balanced by the inertial forces in order to obtain an equation with the proper order of terms. Thus the equation to lowest order in μ takes the form

$$\ddot\beta + \mu C(\psi)\dot\beta + \mu^2 K(\psi)\beta = 0 \qquad (22)$$

The solution of this equation is either a rapid sinusoidal oscillation with frequency of $O(\mu)$, or a sum of exponentials with time constants of $O(\mu^{-1})$, depending on whether the aerodynamic spring is negative or positive (the criterion is a bit more complicated really, but that statement will do for the present discussion). The aerodynamic spring changes sign in the middle of the advancing side and again in the middle of the retreating side, and at each point there is a transition region (of width $O(\mu^{-2/3})$) across which the solutions must be matched. There are also transition regions (of width $O(\mu^{-2/3})$) between the advancing and retreating sides of the disk (near $\psi = 0$ and 180°) through which the solution must be matched; near these points the aerodynamic spring is very small, although it does not change sign. In general, near any point where the aerodynamic spring is very small, the assumption that all terms in Eq. 22 are of the same order is violated, and there must be a narrow transition region about such a point. In this problem there are four such points, dividing the disk into four regions, each with its own main solution. These main solutions may be obtained using the substitution

$$\beta = \exp\left(\int^{\psi} \mu\, p_{-1} + p_0 + \frac{1}{\mu} p_1 + \ldots\, d\psi\right)$$

This substitution gives the main solution (to order p_0) as follows.

$$\beta = |f|^{-\frac{1}{4}} e^{r\left(\mu\frac{\gamma}{12}\cos\psi - \frac{\gamma}{16}\psi\right)} \left\{ C_1 e^{\mu\int^{\psi}\sqrt{f}\,d\psi - r\int^{\psi}\frac{g}{\sqrt{f}}\,d\psi} + C_2 e^{-\mu\int^{\psi}\sqrt{f}\,d\psi + r\int^{\psi}\frac{g}{\sqrt{f}}\,d\psi} \right\} \tag{23}$$

where

$$f = \frac{\gamma}{4}|\sin\psi|\left(\frac{\gamma}{36}|\sin\psi| - \cos\psi - K_p\sin\psi\right)$$

$$g = \frac{\gamma}{6}\left(\frac{1}{4}\cos\psi - K_p\sin\psi - \frac{\gamma}{32}\sin\psi\right)$$

$$r = \begin{cases} +1 & \text{on the advancing side} \\ -1 & \text{on the retreating side} \end{cases}$$

and C_1 and C_2 are constants (if $f < 0$ then C_1 is complex and $C_2 = \overline{C_1}$). There is a main solution of this form for each of the four outer regions of the disk; the solutions are matched through the four transition regions (giving the two constants on one side in terms of the two on the other side) by the standard techniques of perturbation theory.[3,5] By this procedure the transient solution for given initial conditions may be constructed around the entire disk. Floquet theory then gives a quadratic equation for the two roots as follows.

$$\left(e^{\lambda 2\pi + \mu\frac{\gamma}{3}}\right)^2 - 2b\left(e^{\lambda 2\pi + \mu\frac{\gamma}{3}}\right) + 1 = 0 \tag{24}$$

where b is a function of μ, γ, and K_p. The solution for the roots is then

$$\lambda = \begin{cases} -\mu\frac{\gamma}{6\pi} \pm \frac{1}{2\pi}\cosh^{-1} b + ni & \text{for } b > 1 \\ -\mu\frac{\gamma}{6\pi} \pm i\frac{1}{2\pi}\cos^{-1} b + ni & \text{for } -1 < b < 1 \\ -\mu\frac{\gamma}{6\pi} \pm \frac{1}{2\pi}\cosh^{-1}|b| + \frac{i}{2} + ni & \text{for } b < -1 \end{cases}$$

where n is some integer. This result shows the typical behavior of the roots of periodic systems. For $|b| < 1$ the damping is fixed at $-\mu\,(\gamma/6\pi)$ with a change due to b in the frequency; for $b > 1$ the frequency is fixed at n/rev with a positive and negative change due to b in the damping; for $b < -1$ the frequency is fixed at $n + 1/2$/rev with a positive and negative change in the damping. The critical region boundaries are given by $b = 1$ and $b = -1$.

The general character of the critical regions and instability boundaries in the $\gamma - \mu$ plane, as obtained from the solution of Eq. (24), is sketched in Fig. 12. Because μ is large, it happens that $|b|$ is much greater than 1 almost always, so the critical regions dominate the behavior of the roots. The sign of b changes regularly however; b must of course go through zero then, but it does so very quickly, so there is only a very narrow band between the $\mathrm{Im}\lambda = n$/rev and the $\mathrm{Im}\lambda = n + 1/2$/rev regions in which $|b| < 1$. When $|b| < 1$, the real part of λ is $-\mu\,(\gamma/6\pi)$, i.e., the root is stable for all μ and γ; thus there must always be a band of stability surrounding the transition from n/rev to n + 1/2/rev. These characteristics are illustrated in Fig. 12. The locus between the critical regions has a rather fine structure which would be difficult to obtain numerically. A root locus for varying γ or μ (a vertical or horizontal section in Fig. 12) in the vicinity of a critical region boundary would in quick succession move from the RHP (unstable) to the LHP (stable) with frequency fixed at n/rev, rapidly move from $\mathrm{Im}\lambda = n$/rev to $\mathrm{Im}\lambda = n + 1/2$/rev in the RHP with damping given by $-\mu\,(\gamma/6\pi)$ (which would be nearly constant because the critical region boundaries are so close), and then move from the LHP into the RHP with frequency fixed at $n + 1/2$/rev.

Fig. 12 shows that for a given μ the system is stable for a large enough γ. Positive K_p is stabilizing, tending to decrease the size of the instability regions; negative K_p is destabilizing in this sense. The rotating natural frequency of the flap motion, ν, does not enter the high μ case to order p_0 (the aerodynamic spring dominates the centrifugal spring until order p_1); this is consistent with the fact the critical regions dominate the high μ behavior, so the frequency is fixed at a multiple of 1/2/rev.

A comparison of these analytical results with the results of numerical calculations indicates that the high μ solution is good down to $\mu = 2.5$ or so. Thus numerical calculations are required to join the loci from $\mu = 0.5$ to 2.5 say (for γ neither small nor large). The behavior theoretically predicted for the locus at large μ (in particular the rapid movements between $\mathrm{Im}\lambda = n$/rev and $n + 1/2$/rev, and perhaps – for γ not too large – between RHP and the LHP) actually does show up in the numerical calculations of the stability; such behavior of a numerical solution might be questioned without the perturbation solution to provide a guide to what to expect. It is unfortunate that the boundary of the instability region for $\gamma/16$ of order 1 is first encountered at moderate (around $\mu = 2.25$ for small K_p; see Fig. 12) and so cannot be obtained by perturbation techniques (to the order explored anyway). Because of the small time constant in the main solution (of order μ^{-1}) and the four transition regions (of width $O(\mu^{-2/3})$), a numerical calculation of the roots for truly large μ would be difficult; the perturbation theory handles these singular problems analytically, and the

calculations that remain are nonsingular, short, and simple.

A Comparison With Numerical Results

Shown in Fig. 13 are lines of constant $\mathrm{Im}\lambda$ and $\mathrm{Re}\lambda$, for $\nu = 1$ and $K_p = 0$, based on numerical calculation of the eigenvalues of equation (1) using Floquet theory (this figure is taken from Fig. 3 of Ref. 2). Figure 13 should be compared with the analytic results of Fig. 3 (small μ) and Fig. 12 (large μ). The small μ results are good out to about $\mu = 0.5$, which is an excellent range, including all the operating conditions of most helicopters. The large μ results are valid above $\mu = 2.5$ or so, which is also a good range for the perturbation theory. The first high μ instability lobe of Fig. 12 can be seen in Fig. 13, appearing between $\mu = 2.0$ and 2.5

Application of Perturbation Techniques to Helicopter Dynamics

This section returns to the question of whether perturbation techniques might be profitably applied to realistic dynamic systems than the one considered here. As part of the answer, consider what these techniques will not do: obviously they cannot give results for cases where there is no parameter that is either small or large, for example when $\gamma = 16$ and $\mu = 1$. However, the four cases considered together cover a good deal of the ranges of μ and γ, and with primarily analytical results. For many helicopters the small μ case will be quite satisfactory alone. What the techniques can do also includes:

(a) Since they give analytic solutions they provide more insight into the problem, as well as specific design criteria for the system; this feature is particularly important for nonlinear or time-varying systems, which have properties much different from those of constant coefficient, linear systems.

(b) Perturbation methods can find, and handle, cases that are very sensitive to the parameters, or that are difficult to solve accurately by numerical methods.

(c) The methods provide more insight into the rather unusual behavior of the solution of periodic systems, by showing explicitly how the periodic coefficients modify the transient solutions and why they give the root loci their characteristic behavior in the critical regions.

(d) Finally, even if the techniques are not used to find the complete solution, it only takes a little work to find out where the problems are (e.g., critical regions and transition regions) and what the order of things is, which information would be of invaluable help in the numerical analysis of a system.

The extension to more degrees of freedom or more realistic aerodynamic coefficients would certainly make the analysis more complicated. In general however any study – analytic, computational, or experimental – of a system becomes more complicated as the accuracy of the modeling of the true system increases, and perturbation techniques are not expected to be an exception to this rule. Regardless of the system being studied, the position perturbation techniques occupy between simple linear analyses and complex nonlinear numerical calculations makes them a very powerful tool for providing both exact solutions and increasing understanding of problems in rotor dynamics.

There are many problems in rotor dynamics involving nonlinear or periodic coefficients to which perturbation techniques might profitably be applied. Some additional work might be done with the flapping dynamics, considering for example several blades responding to a gust or to shaft motion. The coupled pitch/flap or flap/lag dynamics of a single blade are other important problems of rotor dynamics to which perturbation theory might usefully be applied. While the perturbation solution for small μ will probably be of most interest, there will likely arise problems where other parameters are also useful. As long as a reasonable model is chosen for the system, and as much effort is given to the interpretation of the solution as to its derivation, perturbation techniques should prove quite useful in providing information about these problems, and many others in rotor dynamics and aerodynamics.

This paper has provided examples of the information about dynamic systems which may be obtained using the methods of perturbation theory. The techniques have proved very useful for the problem studied. It should not be concluded however that the techniques used for this problem are all there is to perturbation theory; there are many more methods that have not been touched on here. Perturbation theory is a powerful, and yet not very sophisticated, mathematical technique which should prove very useful in analyzing some of the problems of helicopter dynamics.

References

1. Sissingh, G. J., "Dynamics of Rotors Operating at High Advance Ratios," Journal of the American Helicopter Society, Vol. 13, No. 3, July 1968.

2. Peters, D. A. and Hohenemser, K. H., "Application of the Floquet Transition Matrix to Problems of Lifting Rotor Stability," Journal of the American Helicopter Society, Vol. 16, No. 2, April 1971.

3. Cole, J.D., Perturbation Methods in Applied Mathematics, Blaisdell Publishing Company, Waltham, Massachusetts, 1968.

4. Pearson, C. E., "On a Differential Equation of Boundary Layer Type," Journal of Mathematics and Physics, Vol. 47, No. 2, June 1968.

5. Johnson, Wayne, "A Perturbation Solution of Helicopter Rotor Flapping Stability," NASA TM X-62, 165, 1972 to be published.

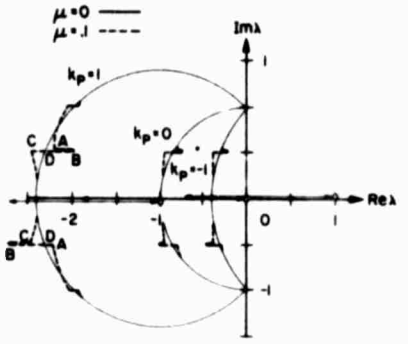

Fig. 1. Foot loci for varying γ, based on the small μ results (to order μ^2); $\nu = 1$ and $\mu = 0$ and 0.1.

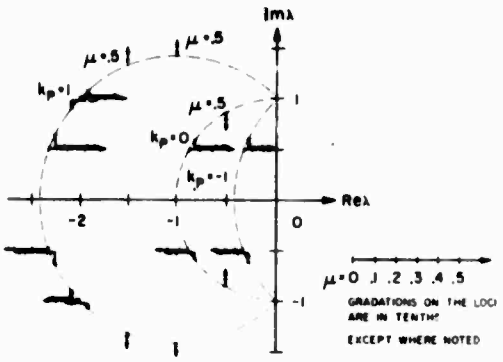

Fig. 2. Root loci for varying μ, based on the small μ results (to order μ^2); γ fixed for each locus ($Re\lambda = -\gamma/16$ for $\mu = 0$)

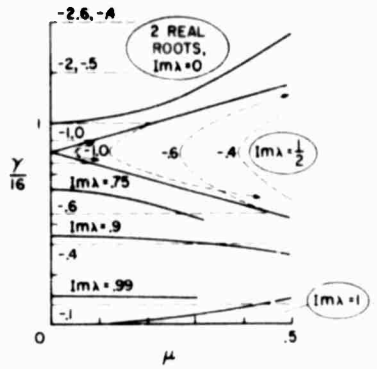

Fig. 3. Lines of constant $Im\lambda$ and $Re\lambda$, based on the small μ results (to order μ^2); $\nu = 1$, $K_P = 0$; ——— $Im\lambda$, – – – – $Re\lambda$, circled values of $Im\lambda$ indicate areas in which $Im\lambda$ is constant

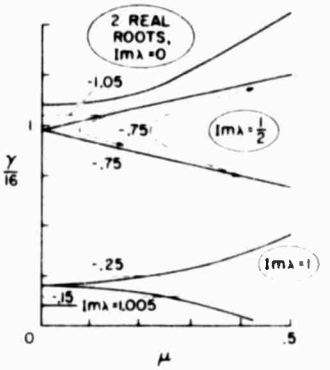

Fig. 4. Lines of constant $Im\lambda$ and $Re\lambda$, based on the small μ results (to order μ^2); $\nu = 1$, $K_P = 0.1$; ——— $Im\lambda$, – – – – $Re\lambda$, circled values of $Im\lambda$ indicate areas in which $Im\lambda$ is constant.

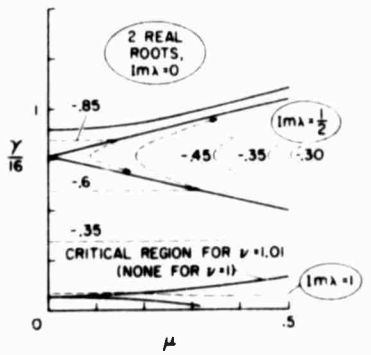

Fig. 5. Lines of constant $Im\lambda$ and $Re\lambda$, based on the small μ results (to order μ^2); $\nu = 1$, $K_P = -0.1$; ——— $Im\lambda$, – – – – $Re\lambda$, circled values of $Im\lambda$ indicate areas in which $Im\lambda$ is constant

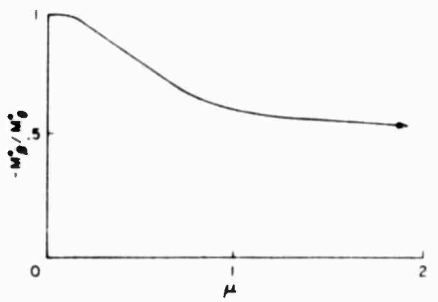

Fig. 6. The ratio $(-M^0_{\dot\beta}/M^0_\theta)$, which governs the effect of K_R and K_P for small ν.

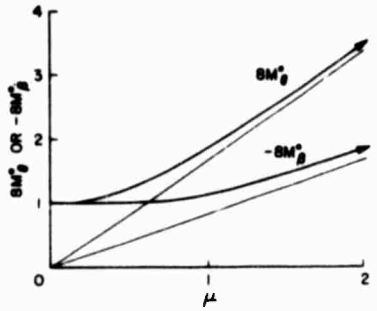

Fig. 7. The averages of the aerodynamic coefficients, which give the roots for small γ.

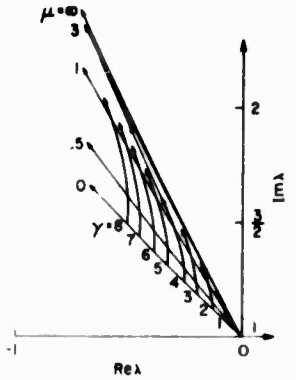

Fig. 8. Root loci for varying μ and γ, based on the small γ results (to order γ); $\nu = 1$ and $K_P = 1$, the effect of the critical regions is not shown.

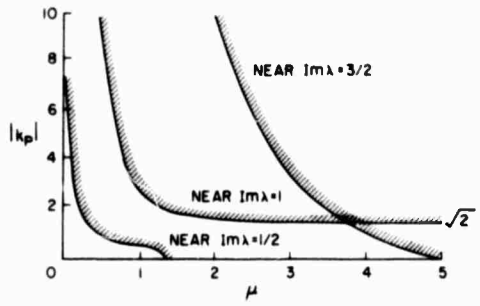

Fig. 9. The K_P vs. μ boundaries for stability in the center of the critical region, based on the small γ results (to order γ); for roots near Imλ = 1/2, 1, and 3/2.

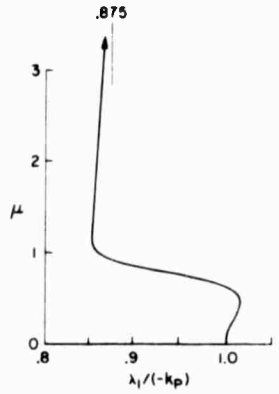

Fig. 10. Motion of the root on the real axis for varying μ, $\gamma = \infty$. For large γ there are two real roots; λ_1 is the finite real root; the other root is at $\lambda = -\infty$ for $\gamma = \infty$.

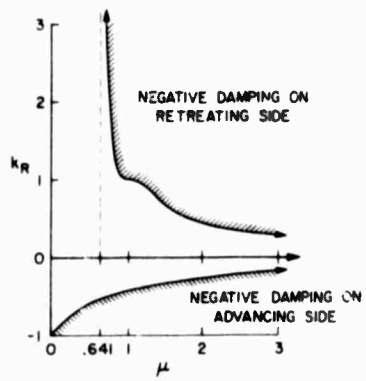

Fig. 11. Flap rate feedback required for negative damping over part of the rotor disk; $-(M_{\dot\beta} - K_R M_\theta) < 0$ (enters into the large γ case).

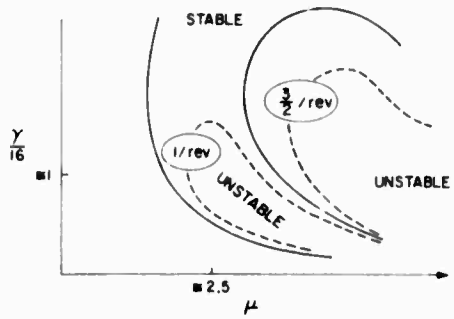

Fig. 12. Sketch of the characteristic behavior of the critical region boundaries and stability boundaries for large μ; ——— boundary of region in which Imλ is fixed at n/rev or n+1/2/rev; — — — — — — boundary of region in which the real part of one root is positive, i.e. unstable.

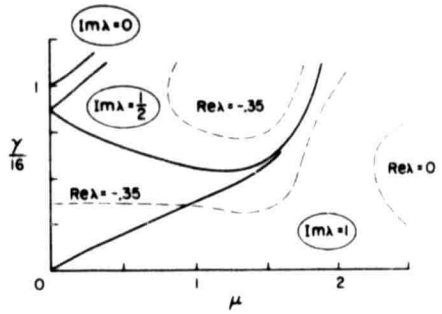

Fig. 13. Lines of constant $\mathrm{Im}\lambda$ and $\mathrm{Re}\lambda$, based on numerical calculation of the eigenvalues (from Ref. 2); $\nu = 1$, $K_p = 0$; ——— $\mathrm{Im}\lambda$, — — — — $\mathrm{Re}\lambda$; circled values of $\mathrm{Im}\lambda$ indicate areas in which $\mathrm{Im}\lambda$ is constant.